

Interplay between the Ionic and Electronic Density Profiles in Liquid Metal Surfaces.

L.E. González¹ D.J. González¹, and M.J. Stott²

¹*Departamento de Física Teórica, Universidad de Valladolid, 47011 Valladolid, SPAIN and*

²*Department of Physics, Queen's University, Kingston, Ontario K7L 3N6 CANADA*

(Dated: June 24, 2021)

First principles molecular dynamics simulations have been performed for the liquid-vapor interfaces of liquid Li, Mg, Al and Si. We analyze the oscillatory ionic and valence electronic density profiles obtained, their wavelengths and the mechanisms behind their relative phase-shift.

PACS numbers: 61.25.Mv, 64.70.Fx, 71.15.Pd

X-ray reflectivity measurements on the surface of liquid metals and alloys, along with other techniques like diffuse scattering or grazing incidence diffraction, have shown the existence of layering in the ionic density profile.^{1,2,3,4,5,6,7,8} Its origin is yet not clear and several reasons have been mooted. Rice and coworkers^{9,10,11} have pointed that the reason for surface layering in metals is the interconnection between the ionic and electronic densities and that the abrupt decay of the electron density at the surface induces an effective wall against which the ions, behaving like hard-spheres, stack. Recently, it has been suggested that surface layering is a rather universal phenomenon, although in most cases it is frustrated by solidification;^{12,13} therefore it only appears in systems whose melting temperature is very low compared with the critical temperature.

The reflectivity experiments probe the total electronic density profile. Therefrom, the ionic density profile is derived by a superposition approximation where the total electron density is taken as the sum of atomic-like electron densities around each of the nuclei in the system. Whereas this approach may be vindicated for the tightly bound core electrons, the case of valence electrons is more subtle. Early calculations of Lang and Kohn for semiinfinite step surfaces¹⁴ showed that the valence electron density does not decay so abruptly, but displays some spill-out outside the surface; moreover inside the bulk it exhibits the so called Friedel oscillations.

Computer simulations of liquid surfaces can evaluate directly the ionic density profile. But only a fully *ab initio* method can deliver an electronic density selfconsistent with the discrete nature of the ions. Orbital based *ab initio* simulations are scarce (just for Si¹⁵ and Na¹⁶) due to the huge computational demands they pose. Orbital free *ab initio* simulations are less demanding, although still expensive, and recent orbital free *ab initio* molecular dynamics (OFAIMD) calculations with 2000 and 3000 particles have studied the surface properties of liquid Li, Na, Na_{0.3}K_{0.7} and Li_{0.4}Na_{0.6}.^{17,18} These studies showed that the superposition approximation produces a valence electronic density profile very similar to the fully selfconsistent one, except for the width of the interface due to the spill-out.

This communication reports results for the liquid-vapor interface of liquid Li, Mg, Al and Si near their respective melting points. The calculations were per-

Metal	ρ (\AA^{-3})	T (K)	L (\AA)	d (\AA)	δ (\AA)	E_{cut} (Ryd)
Li	0.0445	470	28.44	55.55	16	9.50
Mg	0.0383	953	29.90	58.41	16	8.50
Al	0.0529	943	28.97	45.05	14	11.25
Si	0.0555	1740	27.41	47.96	20	15.55

TABLE I: Thermodynamic states and simulation details.

formed by the OFAIMD method where the forces acting on the nuclei are computed from electronic structure calculations, based on the density functional theory (DFT), which are performed as the ionic trajectories are generated. In OFAIMD¹⁹ the energy and forces acting on a system of N ions are computed from the ground state energy and density of the valence electrons, which interact with the ions through suitable local pseudopotentials. According to DFT the ground state electron density for a given ionic configuration minimizes an energy functional which is the sum of the electronic kinetic energy, the classical electrostatic energy, the energy of interaction with the ions through local pseudopotentials, and the exchange and correlation energy, for which we use the local density approximation. The keynote of the OFAIMD simulations is the use of an explicit, but approximate, kinetic energy functional. Another basic magnitude is the local pseudopotential, $v_{ps}(r)$, describing the ion-electron interaction. It has been developed from first principles by fitting to the displaced electronic density induced by an ion immersed in a metallic medium. Further details on the method appear in references [20,21].

The application of this formalism to bulk liquid Li, Mg and Al^{20,21} has provided an accurate description of their static and dynamic properties. Recent calculations for bulk liquid Si²² have yielded a good description of the static structure factor (i.e. peak positions and amplitudes as well as the shoulder at the high- q side of the main peak); moreover, the number of neighbors is around 6, as in the experiment, while the diffusion coefficient is in the same range as other *ab initio* results.

The simulations proceed as follows: given the ionic positions at time t , the electron density is expanded in plane waves with energy less than a given cutoff, E_{cut} , and the energy functional is minimized with respect to the plane wave coefficients, yielding the ground state elec-

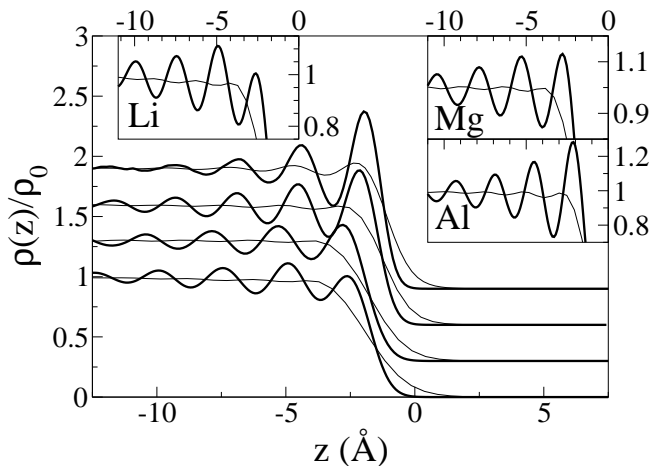


FIG. 1: Normalized ionic (thick line) and valence electronic (thin line) density profiles normal to the liquid-vapor interfaces. The Mg, Al and Si data are shifted upwards by 0.3, 0.6 and 0.9 units. The insets highlight the region near the surface to enhance the valence electronic density oscillations.

tronic density and energy, and the forces on the ions, based on which the ionic positions and velocities are updated. For all the systems, the associated density profiles were computed based on a sample of 20000 configurations. The simulation setup consists of a periodically repeated supercell with dimensions $L \times L \times L_z$, and a liquid slab of 2000 particles placed initially in the center of the supercell, occupying a volume consistent with the experimental densities at the temperatures considered, and two free surfaces normal to the z axis. In all cases the distance, d , between the two surfaces is greater than 45 Å and the distance, $\delta = L_z - d$, between the periodically repeated slabs is greater than 14 Å, which are enough to guarantee the absence of unwanted interactions between the slabs and between the two surfaces of one slab. Table I summarizes these data and other simulation details.

The longitudinal ionic density profiles were computed from a histogram of particle positions relative to the slab center of mass and the results are depicted in figure 1. All systems show stratification for around four layers into the bulk liquid, which agrees with the experimental observations in other liquid metals. The wavelength of the ionic oscillations, λ , shows a good scaling with the radii of the associated Wigner-Seitz spheres, R_{WS} ; however no clear relationship with electronic parameters, like the radii per electron, r_s , has been found (see figure 2, where we also include data for other systems studied within the same method). This fact suggests that the ionic oscillations are not induced by the Friedel oscillations in the electronic density, but they are primarily due to atomic stacking against the interface. The relative amplitude of the outermost oscillation increases with the valence and we attribute it to the drastic decrease undergone by the valence electronic density at the interface, which induces a steeper potential wall when moving from Li to Si.

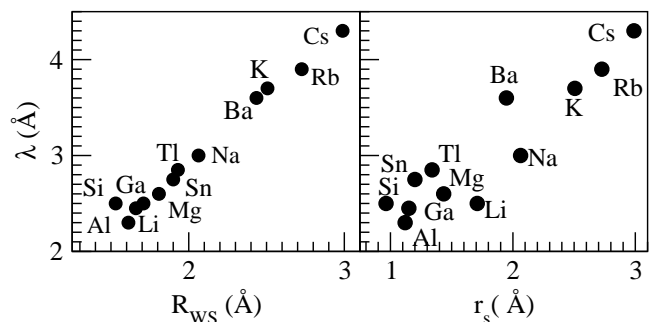


FIG. 2: Wavelength of the oscillations in the density profiles as a function of the Wigner-Seitz radius and r_s , the radius of a sphere which on average contains one electron.

The self-consistent valence electronic density profiles are shown in figure 1. They oscillate near the surface although with a much smaller amplitude than the ionic ones. However, their relative phase exhibits an interesting behavior, which evolves from being in opposite phase for Li to almost in phase for Si. An opposite phase between the ionic and the valence electronic oscillations had already been obtained in the Monte Carlo simulations of the interface of liquid alkalis⁹ and Ga.¹⁰ (see figures 7-9 in reference [9] and figure 11 in reference [10]). This behavior was attributed to the competition between the electronic kinetic energy contribution, which gets smaller values by weakening the oscillations, and the interaction term between electrons and ions, which being attractive takes smaller values for in-phase oscillations. An opposite phase was also found in OFAIMD simulations for the liquid-solid interface of Al,²³ and it was justified in terms of the interaction (represented by the use of a pseudopotential), between valence and core electrons, which tends to expel the valence electrons from the ionic positions. Indeed, the idea that the ionic and valence electron profiles oscillate in opposite phase appears widely accepted; however a closer scrutiny reveals some moot points: (i) the magnitude of the electronic kinetic energy is too small in comparison with the ion-electron interaction term (about 1%), so as to ascribe it a prime role in establishing the phase of the oscillations, and (ii) when (some of) the valence electrons are s -type a maximum of the valence electron pseudodensity is found at the ionic position (see the inset of figure 3). Therefore, we have performed several tests to clarify the reasons underlying the phase-shift between the ionic and valence electronic density profiles.

First a valence electron density profile was generated by superposing at ion sites pseudoatomic valence densities as obtained in the pseudopotential construction. This amounts to a linear response treatment of the valence electron density and therefore lacks any trace of the kind of competition argued above. These valence electron density profiles for Li and Si are compared with the self-consistent OFAIMD profiles in figure 3, and there

is very good agreement. In particular the phase of the valence electron density oscillations is reproduced, which suggests that the phase difference between the ionic and valence electron density profiles is connected to some feature of the pseudoatom density. The pseudoatom densities projected onto the z -axis, are also shown in figure 3. The main features are the width and the presence of weak Friedel oscillations. To clarify the possible influence of these features on the phase of the electron density profile we have fitted the projected pseudoatom density to a model with no Friedel oscillations. A good fit is obtained for a model density of the normalized form $\exp[-|z/\sigma|^3]$, which includes only a width parameter, σ , with values: 1.60, 1.50, 1.29 and 1.13 Å for Li, Mg, Al and Si respectively. Superposing these model densities at the ionic positions generated by the simulations gives valence electron density profiles which, for all systems, are rather similar to the self-consistent OFAIMD ones, as shown in figure 3 for Li and Si. Again, the phase of the oscillations is preserved, and it is inferred that the Friedel oscillations in the valence pseudodensity are not responsible for the phase difference. The reason for the phase difference between ion and valence electron density profiles must lie in the width of the pseudoatom density as compared with the separation of layers in the ionic density profile. The ratio σ/λ has values 0.64, 0.58, 0.55 and 0.45 for Li, Mg, Al and Si respectively, correlating with a decreasing phase difference between the ion and electron oscillations. Moreover, the OFAIMD results for other liquid metals near melting (Na, K, Rb, Cs, Ba, Ga, Tl, Sn) show a correlation between the phase difference and the ratio σ/λ . The systems fall into groups with similar phase differences: (i) the alkalis ($0.62 \leq \sigma/\lambda \leq 0.64$), (ii) Mg and Ba (0.58 and 0.59), (iii) Al (0.55) and (iv) Tl, Ga, Si and Sn ($0.45 \leq \sigma/\lambda \leq 0.46$).

We stress that the width of the pseudoatomic density is characteristic of the atomic species, whereas the interlayer distance in the ionic profile, λ , depends on the environment. For example, in the liquid-vapor interface of Al $\lambda = 2.35$ Å, whereas in contact with the (100) face of its solid fcc phase²³ $\lambda \approx 2.1$ Å (which is close to the interlayer distance in the solid) and leads to a ratio $\sigma/\lambda \approx 0.613$, well within the range of the out-of-phase oscillations. To reinforce this argument we have taken the ionic positions of the liquid Al slab, and superposed the model pseudoatom densities with different widths, namely, $\sigma = 1.60, 1.29$ and 1.00 , with corresponding $\sigma/\lambda = 0.68, 0.55$ and 0.43 respectively. Figure 4 shows the resulting model valence electron density profiles which evolve from opposite phase in the wider model to in-phase for the narrower one.

The total electron density profile, which is the quantity accessible to experiment, is obtained by the sum of the self-consistent OFAIMD valence electron density profile plus the superposition of core electron densities, and is shown in figure 5. Since the core densities are rather narrow their superposition gives a profile in phase with the ion density profile. Consequently, when the valence elec-

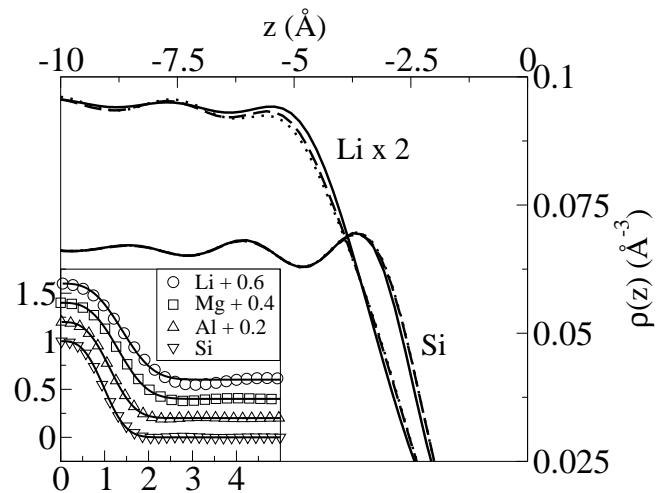


FIG. 3: Valence electron density profiles at the liquid-vapor interfaces. The continuous line is the self-consistent result, the dashed line represents the linear superposition of pseudoatomic densities, and the dotted line is the superposition of model densities without Friedel oscillations. The inset shows the projected pseudoatom electron densities (symbols) together with the fit to the model proposed in the text (lines).

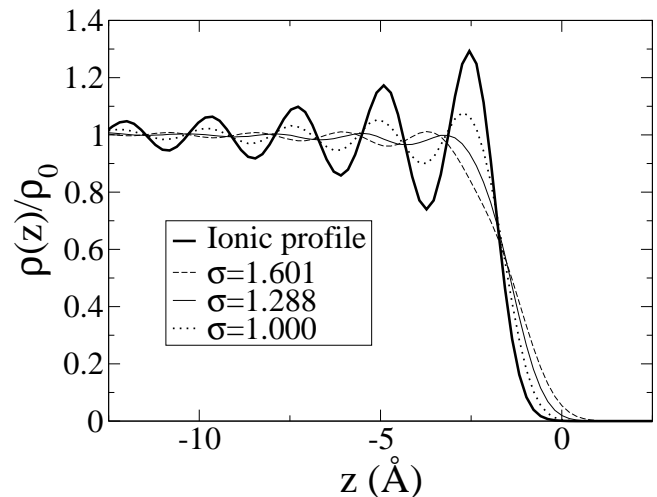


FIG. 4: Normalized ion and valence electron densities of liquid Al obtained by superposition of several model densities of different widths, σ .

tron density is added the phase of the total electron density profile depends on the relative weight of the core electron (always in phase) and valence electron (any phase is possible) contributions. In this respect liquid Li is the most interesting case, since the valence contribution (in opposite phase) is 1/3 of the total while the core contribution (in phase) is 2/3. Figure 5 shows that the core contribution dominates even for Li, and the total electron density profile is in phase with the ionic one.

In summary, 20000 configurations of 2000-particle

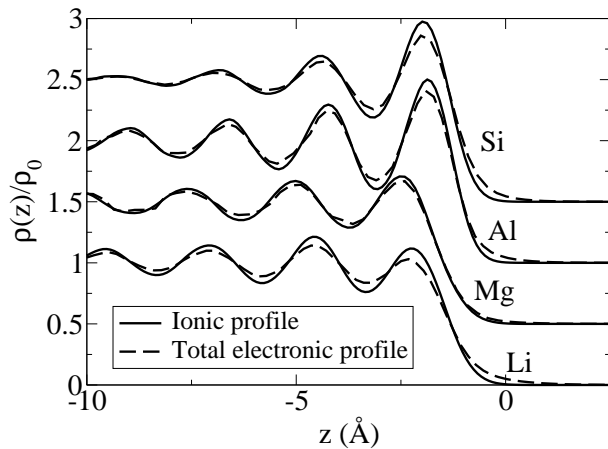


FIG. 5: Normalized ion profile and total (core + valence) electron densities for the systems studied. The Mg, Al and Si data are shifted upwards by 0.5, 1 and 1.5 units respectively.

slabs have been simulated *ab initio* using the OFAIMD method to obtain the ionic and valence electron density profiles of the liquid-vapor interfaces of Li, Mg, Al and Si; results have also been obtained and are reviewed here for some other systems. All the ionic profiles show layering. The oscillations in the ionic profile are not induced by Friedel oscillations in the electron profile, but are due to atomic stacking. The valence electron density profiles also show oscillations, but the phase with respect to the ion profiles evolves following a pattern that correlates directly with the ratio between the width of the pseudoatoms and the wavelength of the ionic oscillations. Nevertheless, the total electron density profile, even for Li, oscillates in phase with the ion profile, being dominated by the more localized and numerous core electrons.

The financial support of the DGICYT of Spain (MAT2002-04393-C0201) and the NSERC of Canada is acknowledged.

-
- ¹ O. M. Magnussen et al., Phys. Rev. Lett. **74**, 4444 (1995).
² M. Regan et al., Phys. Rev. Lett. **75**, 2498 (1995).
³ M. J. Regan et al., Phys. Rev. B **55**, 15874 (1997).
⁴ H. Tostmann et al., Phys. Rev. B **59**, 783 (1999).
⁵ H. Tostmann et al., Phys. Rev. B **61**, 7284 (2000).
⁶ E. DiMasi et al., Phys. Rev. Lett. **86**, 7538 (2001).
⁷ O. Shpyrko et al., Phys. Rev. B **67**, 115405 (2003).
⁸ O. G. Shpyrko et al., Phys. Rev. B **70**, 224206 (2004).
⁹ D. Chekmarev, M. Zhao and S. A. Rice, J. Chem. Phys. **109**, 768 (1998)
¹⁰ M.S. Zhao, D.S. Chekmarev, Z.H. Cai and S. A. Rice, Phys. Rev. E **56**, 7033 (1997)
¹¹ S. A. Rice, Mol. Simul. **29**, 593 (2003), and references therein.
¹² E. Chacón et al., Phys. Rev. Lett. **87**, 166101 (2001).
¹³ E. Velasco et al., J. Chem. Phys. **117**, 10777 (2002).
¹⁴ N. D. Lang and W. Kohn, Phys. Rev. B **1**, 4555 (1970).
¹⁵ G. Fabricius et al., Phys. Rev. B **60**, R16283 (1999).
¹⁶ B. G. Walker, C. Molteni, and N. Marzari, J. Phys.: Condens. Matter **16**, S2575 (2004).
¹⁷ D. J. González, L. E. González, and M. J. Stott, Phys. Rev. Lett. **92**, 085501 (2004).
¹⁸ D. J. González, L. E. González, and M. J. Stott, Phys. Rev. Lett. **94**, 077801 (2005).
¹⁹ M. Pearson, E. Smargiassi, and P. A. Madden, J. Phys.: Condens. Matter **5**, 3221 (1993).
²⁰ L. E. González, D. J. González, and J. M. López, J. Phys.: Condens. Matter **13**, 7801 (2001).
²¹ D. J. González et al., Phys. Rev. B **65**, 184201 (2002).
²² A. Delisle et al., unpublished (2005).
²³ B. J. Jesson and P. A. Madden, J. Chem. Phys. **113**, 5935 (2000).